



Hypofunction of directed brain network within alpha frequency band in depressive patients: a graph-theoretic analysis

Shuang Liu² · Sitong Chen¹ · Zhenni Huang³ · Xiaoya Liu² · Meijuan Li³ · Fangyue Su¹ · Xinyu Hao² · Dong Ming^{1,2}

Received: 23 March 2021 / Revised: 4 December 2021 / Accepted: 8 January 2022 / Published online: 5 February 2022
© The Author(s) 2022

Abstract

Directed brain networks may provide new insights into exploring physiological mechanism and neuromarkers for depression. This study aims to investigate the abnormalities of directed brain networks in depressive patients. We constructed the directed brain network based on resting electroencephalogram for 19 depressive patients and 20 healthy controls with eyes closed and eyes open. The weighted directed brain connectivity was measured by partial directed coherence for α , β , γ frequency band. Furthermore, topological parameters (clustering coefficient, characteristic path length, and et al.) were computed based on graph theory. The correlation between network metrics and clinical symptom was also examined. Depressive patients had a significantly weaker value of partial directed coherence at alpha frequency band in eyes-closed state. Clustering coefficient and characteristic path length were significantly lower in depressive patients (both $p < .01$). More importantly, in depressive patients, disruption of directed connectivity was noted in left-to-left ($p < .05$), right-to-left ($p < .01$) hemispheres and frontal-to-central ($p < .01$), parietal-to-central ($p < .05$), occipital-to-central ($p < .05$) regions. Furthermore, connectivity in LL and RL hemispheres was negatively correlated with depression scale scores (both $p < .05$). Depressive patients showed a more randomized network structure, disturbed directed interaction of left-to-left, right-to-left hemispheric information and between different cerebral regions. Specifically, left-to-left, right-to-left hemispheric connectivity was negatively correlated with the severity of depression. Our analysis may serve as a potential neuromarker of depression.

Keywords Depression · Alpha frequency band · Partial directed coherence · Weighted directed brain network · Disruption of directed connectivity · Correlation

Introduction

Characterized by high level of anhedonia and continuous pessimism (DeRubeis et al. 2008; Kessler et al. 2003), depression is one of the most serious and also common mental disease. According to the World Health Organization, there are about 350 million persons in the world suffering from depressive disorders. However, the pathological mechanism of depression is still not clear, and the methods of clinical diagnosis of depression are somewhat subjective (Hulshoff Pol and Bullmore 2013), which has brought serious psychological and economic burden to people. It is imperative to explore the pathological functional mechanism of this mental disorder to improve its detection and treatment efficiency. With the development of brain imaging technology, researchers have found that human brain is one of the most complex systems in nature,

Shuang Liu, Sitong Chen have contributed equally to this work.

✉ Dong Ming
richardming@tju.edu.cn

Shuang Liu
shuangliu@tju.edu.cn

¹ School of Precision Instruments and Optoelectronics Engineering, Tianjin University, Tianjin, China

² Academy of Medical Engineering and Translational Medicine, Tianjin University, Tianjin, China

³ An Ding Hospital, Tianjin, China

in which a large number of neurons form a highly complex network to enable information processing and cognitive expression (Bassett and Bullmore 2006). Brain networks can contribute to understanding the structure, function, and pathological mechanisms of the brain, which can help prevent, diagnose, and treat mental diseases.

Findings with a specific focus on brain networks have revealed that the structural and functional networks of human brain conform to a complex network model (Bullmore and Sporns 2009; van den Heuvel and Hulshoff Pol 2010). Graph theory provides a promising tool to explore computational models of brain networks and quantitatively describes the connectivity of different brain regions (Kaiser 2011; Mikail Rubinov and Sporns 2010). As a common analytical approach for complex systems, such as human brain, graph theory has indeed been applied to explore the functional and structural abnormalities in mental disorders, such as depression, Alzheimer's disease, schizophrenia, and bipolar disorder (Leistedt et al. 2009; Micheloyannis et al. 2006; Rubinov et al. 2009; Stam et al. 2006, 2008; Strakowski et al. 2012). The topological network parameters are typically evaluated to quantify the properties of these mental disorders, which then provide the diagnostic criteria at the global and local levels. Recently, alterations in the structure and functions of brain networks have been frequently discovered in depressive patients (DP) using graph theory (Stam and Reijneveld 2007). For example, an electroencephalogram (EEG)-based study revealed that DP showed significant randomization of global network metrics; they were characterized by lower characteristic path length at the delta and theta bands compared with healthy controls (HC) (Leistedt et al. 2009). A study based on resting state functional magnetic resonance imaging (fMRI) data from DP also found a decrease in characteristic path length, an increase in global efficiency, and changes in other metrics, such as reduced clustering coefficient and local efficiency (Li et al. 2017). In another study, researchers constructed the brain functional network by collecting task-state fMRI data of 13 major depressive disorder (MDD) patients and found that the global efficiency of the brain functional network decreased and the local efficiency increased when MDD patients performed negative and neutral emotion processing tasks (Park et al. 2014). The decreased global efficiency of the dorsal striatum, inferior frontal gyrus, orbitofrontal cortex, occipital lobe, and somatosensory cortex in MDD patients was also shown in an fMRI-based study (Meng et al. 2014).

However, conventional structural or functional network analysis considers only the undirected information connectivity, whereas the transmission of information in the brain appears to be directed. For example, a preferential direction of information flow was found in the delta and beta rhythms across wake to sleep states: preferred right-to-

left hemisphere direction for delta and left-to-right for beta rhythms (Bertini et al. 2007). Consequently, studies about information flow, especially the directed connectivity between different cerebral hemispheres as well as cerebral regions, may contribute to uncovering more information about the functions and the structure of the brain. Previous studies have suggested that the interactions between the left and right cerebral hemispheres play a crucial role in cognitive and emotional processing, which contributes to mediating the symptoms of depression (Banich et al. 1992; Compton et al. 2005; Toro et al. 2008). Besides, it is also necessary to investigate the functional coordination of different cerebral regions. For instance, the frontoparietal control systems contribute to promoting and maintaining mental health (Cole et al. 2014). Directed analysis may have considerable impact on the studies for dysfunctions of DP. To our knowledge, few studies have yielded some results on depression through directed network research. The directed functional connectivity between cerebral hemispheres and between different cerebral regions is still not clearly known. To generalize the study of directed functional connectivity, effective connectivity, which deals with causal interactions of brain regions, can be used to address this obstacle. Partial directed coherence (PDC) is one of the main methods used to quantify the effective connectivity between different channels. It neglects the cross-channel directed interdependence that can be extracted from multivariate data. This cortical interdependence is essential to understanding inter- and intra-hemispheric as well as different regions' causal interactions (Sun et al. 2008). Indeed, PDC has been used to simulate a neural network to help further research about the functions of brain because of its ability to reveal the direction of information flow (Sameshima and Baccalá, 1999). This is a promising tool to study the aberration of directed functional connectivity in various brain disorders (Coito et al. 2016; Ana Coito et al. 2019; Sperdin et al. 2018).

To investigate alterations of the directed connectivity and the topological network parameters in DP, we explored differences in the weighted directed functional brain network between DP ($N = 19$) and HC ($N = 20$) in resting state with eyes closed (EC) and eyes open (EO). We first examined the differences of the mean value of partial directed coherence over all paired channels between the two groups. Then, graph theory was applied to construct the weighted directed network for subsequent analysis. Conventional topological parameters including the clustering coefficient, characteristic path length and global efficiency were computed. What's more, we presented the inter- and intra-hemispheric connectivity matrices and statistical significance of different groups as well as the significant differences of directed connectivity between cerebral regions. In addition, the differences in the local

characteristics between the two groups were compared, namely, local efficiency and out- and in-strength. Furthermore, the Pearson correlation coefficients between depression symptom measures and network metrics were computed. We hypothesized abnormalities in topological parameters and a disrupted connectivity of different cerebral hemispheres and regions in DP compared with HC.

Methods

Subjects

Depressive patients ($N = 19$) and healthy controls ($N = 20$) with no prior or current history of depression were recruited to participate. All of them were right-handed. The age of depressive patients (female/male = 11/8) ranged from 21 to 31 years (mean = 26.53; standard deviation (SD) = 3.49), and the age of healthy controls (female/male = 11/9) ranged from 21 to 31 (mean = 25.00; standard deviation = 2.29). There were no significant between-group differences in age ($t = -1.6233, p = .1130$) or gender ($\chi^2 = .0332, p = .8554$).

Depressive patients from Tianjin An Ding Hospital, Tianjin, China and The Second Xiangya Hospital, Changsha, China were diagnosed and recommended by two clinical psychiatrists. The healthy controls were all recruited from Tianjin University. The study was approved by the Ethics Committee of Tianjin An Ding Hospital and the Ethics Committee of The Second Xiangya Hospital. All patients received a Structured Clinical Interview for Diagnostic and Statistical Manual of Mental Disorders (DSM)-IV. The inclusion criteria for depressive patients were consistent with DSM-IV criteria: Hamilton Depression Rating Scale (HDRS) scores of 17 or greater on the 17-item scale. All the patients were first-episode untreated.

Exclusion criteria were the following: previous history of psychiatric genetic disorders or other psychiatric diseases, severe physical diseases, other medical drugs before the trial, intellectual or behavioral disorders, a history of alcohol and drug abuse, and participating in clinical trials of other drugs.

Experiment

This study was conducted on the basis of an 8 min resting state experiment that was performed in a quiet environment without exogenous interference. The procedure of the study was clearly explained to all subjects. During the experiment, each subject was prompted to remain quiet and relaxed with their eyes open and eyes closed in two alternating orders by voice playback.

EEG recordings and preprocessing

Left ear mastoid process (M1) was selected as the reference electrode, and the EEG data of 30 conductive electrodes were finally recorded using the Neuroscan SYNAMPS based on the international 10–20 system (30 channels = FP1, FP2, FZ, F4, F8, F3, F7, FCZ, FC4, FT8, FC3, FT7, CZ, C4, T8, T7, C3, TP7, TP8, P7, CPZ, CP4, CP3, PZ, P4, P8, P3, OZ, O2, and O1). Sampling frequency was 1000 Hz, and the channel impedances were maintained less than 10 k Ω .

EEG preprocessing was performed using EEGLAB in MATLAB (R2016a), which is an open-source MATLAB-based toolbox for data processing of EEG signals. First, the data were re-referenced against the binaural mean reference (M1 and M2). The signals were band-pass filtered within 0.1–100 Hz and then down-sampled to 500 Hz. The 8 min signals were extracted into two sections: 4 min eyes open and 4 min eyes closed. Finally, independent component analysis (ICA) was used to remove signal artifacts caused by eye movements and breathing. We used the ADJUST1.1 toolbox in EEGLAB to help remove the artifacts, which can help users automatically filter out unnecessary ICA components and reduce errors caused by insufficient prior knowledge (Mognon et al. 2011). Frequency bands of interest were classified by alpha (8–13 Hz), beta (13–30 Hz) and gamma (30–50 Hz) respectively.

Partial directed coherence for EEG connectivity

PDC was computed between all pairs of EEG channels at each frequency band as a measure of directed functional connectivity. PDC is a frequency-domain approach to describe directed interactions among multivariate time series. It is a normalized index showing the degree of directional linear interdependence between pairs of variables at each frequency (Sameshima and Baccalá 1999). In a linear framework, the notion of Granger-causality is closely related to vector autoregressions. The mathematical details of PDC can be briefly described as follows.

EEG is taken as an example to explain. Assume that the original EEG is a matrix of K channels:

$$Y(n) = [y_1(n), \dots, y_K(n)]^T$$

$y_i(n)$ represents the EEG signal in channel i . Then, a vector autoregressive (van den Heuvel and Hulshoff Pol) model of order p for $Y(n)$ is defined as

$$Y(n) = \sum_{r=1}^p A_r Y(n-r) + E(n)$$

where A_r is the calculated $K * K$ coefficient matrix of the model using ARfit, a toolbox of Matlab (Schnieder and

Neumaier 2001). $E(n)$ is the error between the current value and the predicted value. Next, a representation of Granger causality in the frequency domain can be obtained from the Fourier transform of A_r (Baccalá and Sameshima 2001)

$$A(f) = I - \sum_{r=1}^p A_r e^{-i2\pi fr}$$

In this case, the equation denotes the difference between the n -dimensional identity matrix I and the Fourier transform of the coefficient series. Then the PDC value of channel j to channel i is defined as $PDC_{j \rightarrow i}(f) = |A_{ij}(f)|$

$\left/ \sqrt{\sum_k |A_{kj}(f)|^2} \right.$. $PDC_{j \rightarrow i}$ represents the ratio of information flowing from j to i to all information flowing from j . Simply put, the PDC value reflects the influence of channel j on channel i , which accounts for the proportion of its influence on other channels.

Construction of the weighted directed brain network

We constructed the brain network using graph theory. The network was represented by a matrix with N nodes and K edges, where nodes indicated the electrodes and edges indicated the value of PDC. In this study, we got 30 electrodes. PDC was computed for every pair of electrodes for every subject in every frequency band. After calculating the value of PDC of each subject in the different groups, the PDC matrix A_{ij} ($i, j = 1, 2, \dots, M$; here $M = 30$) was obtained. The diagonal of each PDC matrix was set to 0. Therefore, there were 39 matrices (30×30) for 39 subjects totally. The weighted directed brain network could be plotted based on these PDC matrices. The element a_{ij} in the PDC matrix indicated the weights of edges from the j th electrode to i th electrode. The mean directed functional brain network graph of each group was eventually obtained.

Network analysis

Five common graph theory metrics were used to analyze the properties of the network. All of these graph theory metrics were calculated by Brain Connectivity Toolbox (Mikhail Rubinov and Sporns 2010).

The weights of edges connecting to a node i is called the strength W_i . The higher the strength of a node, the more important it is. In a directed graph, the strength is divided into in-strength (the weights of edges that flow from other nodes to the node) and out-degree (the weights of edges that flow out of the node).

$$W_i = \sum_j w_{ij}$$

The clustering coefficient C is used to describe the extent of clustering between nodes in a graph. The clustering coefficient C_i of a node i is defined as the number of existing edges between neighbors of i divided by the maximum possible number of edges between neighbors. The average C_i of all nodes is C ,

$$C = \frac{1}{n} \sum_i \frac{1}{2} \frac{[(P^{[1/3]}) + (P^T)^{[1/3]}]_{ii}^3}{[k_i(k_i - 1) - 2 \sum a_{ij} a_{ji}]}$$

where $P^{[1/3]}$ is defined as $\{w_{ij}^{1/3}\}$, i.e., the matrix obtained by taking the 3rd root of each entry (Fagiolo 2007), and k_i is defined as the sum of all edges connected to node i .

Another parameter is the characteristic path length L . It is a global characteristic that indicates how easy it is to transport information in the network. The characteristic path length L is usually defined as the mean of the shortest path lengths between all possible pairs of nodes,

$$L = \frac{1}{n} \sum_i \frac{\sum_j d_{ij}^w}{n - 1}$$

where d_{ij}^w is the shortest weighted path length (distance) between nodes i and j .

However, this original definition of L is problematic in networks that comprise more than one component because there exist nodal pairs that have no connecting path. A harmonic mean distance is used to measure L , which is called the global efficiency G_e (Achard and Bullmore 2007; Stam and Reijneveld 2007). G_e is also used to describe the global characteristics. The local efficiency L_e , defined as the mean of the efficiencies of all subgraphs of neighbors of each of the nodes of the graph, is used to describe the local characteristics.

$$L = \frac{1}{n} \sum_i \frac{\sum_j (d_{ij}^w)^{-1}}{n - 1}$$

Statistical analysis

The normality of data was checked using the Kolmogorov–Smirnov test. All of the data were normally distributed, thus inter-group comparisons of network metrics were conducted with t-test. Any test that yielded a p -value of 0.05 or less were considered statistically significant at an alpha level of 0.05. The Benjaminiand-Hochberg false discovery rate correction (BH-FDR) was performed to correct the p -value (Benjamini and Hochberg 1995).

Results

Partial directed coherence per frequency band in EO state and EC state

Since eyes-open and eyes-closed state could exert an influence on the EEG oscillation, the mean values of PDC (averaged over all pairwise combinations of channels) at different frequency bands (alpha, beta, and gamma) were first calculated in both EO state and EC state, shown in Fig. 1. As can be seen, DP tended to show a lower value of PDC at all frequency bands in EC state, whereas there was no such trend in EO state. However, the significant difference after BH-FDR correction was only found at alpha band in EC state, where DP had a significantly lower value of PDC than HC (0.1176 ± 0.0069 versus 0.1283 ± 0.0108 , $t = 3.6682$, $corrected p = .0050$). There was no significant difference between DP and HC at the beta (0.1336 ± 0.0067 versus 0.1378 ± 0.0085 , $t = 1.6990$, $corrected p = .0979$) and gamma (0.1304 ± 0.0081 versus 0.1356 ± 0.0076 , $t = 2.0323$, $corrected p = .0743$) frequency bands in EC state. Consequently, it was the alpha band in EC state that was the condition with the best discrimination.

Mean weighted directed brain network graph and its topological parameters

The mean PDC matrices were then converted to weighted directed brain network graphs at the alpha band in EC state. Mean brain network graphs for DP and HC are depicted in Fig. 2, in which the connectivity weights between channels greater than 0.172 are retained for easy observation. As can be seen, the brain disconnection phenomenon was observed

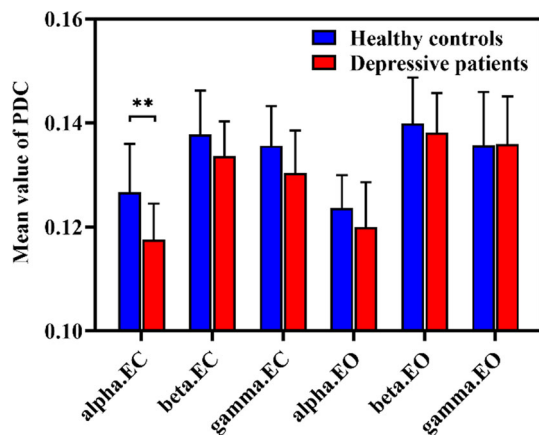


Fig. 1 The mean value of PDC at the alpha, beta, and gamma frequency bands in EC state and EO state. The mean and standard deviation are represented by bars and lines, respectively, with blue for healthy controls and red for depressive patients. The asterisks denote corrected $p < .01$ (t-test)

in the depressive group. Then C , G_e , and L were calculated to quantify the metrics of the graph, shown in Fig. 3. It is obvious that DP showed a significant (after correction) lower value for C and L (C , 0.0997 ± 0.0090 versus 0.1147 ± 0.0169 , $t = 3.4974$, $corrected p = .0023$; L , 0.0722 ± 0.0199 versus 0.0960 ± 0.0305 , $t = 2.8989$, $corrected p = .0050$). This indicated a more random network structure in DP.

Inter-hemispheric and intra-hemispheric functional connectivity

To assess the alterations of information flow in depressive patients, we computed the mean inter-hemispheric and intra-hemispheric directed functional connectivity. 30 channels were divided into two parts, left hemisphere and right hemisphere. As depicted in Fig. 4, the matrix consists of four quadrants, of which the first quadrant indicates left-to-right (LR) hemisphere, the second indicates right-to-right (RR) hemisphere, the third indicates left-to-left (LL) hemisphere, and the fourth indicates right-to-right (RL) hemisphere. Obviously, the connectivity was disrupted in DP in both the inter-hemispheric (RL) and intra-hemispheric (LL) interactions. To evaluate quantitatively, the inter- and intra-hemispheric connectivity strength of each subject was then calculated and the statistical tests with BH-FDR correction were performed between two groups. As shown in Fig. 5, the DP had lower inter-hemispheric and intra-hemispheric connectivity compared with the HC, especially for LL (17.44 ± 3.62 versus 19.52 ± 2.59 , $t = 2.0540$, $p = .0481$) and RL (15.64 ± 4.91 versus 20.53 ± 3.47 , $t = 3.5744$, $p = .0023$) connectivity. This demonstrates that depression may interfere with the interactions inside the left hemisphere as well as from the right hemisphere to the left, which may be related with the left hemisphere asymmetry caused by the cortical deactivation of the right cerebral hemisphere reported in a prior study (Haag et al. 1994).

Directed connectivity between different cerebral regions

Further, we also explored the connectivity strength between different cerebral regions. Thirty channels were divided into 5 regions: frontal (F, FP1, FP2, F7, F3, FZ, F4, F8), temporal (T, FT7, T7, TP7, FT8, T8, TP8), central (C, FC3, FCZ, FC4, C3, CZ, C4, CP3, CPZ, CP4), parietal (P, P7, P3, PZ, P4, P8), and occipital (O, O1, OZ, O2). The directed connectivity of each subject between different regions was calculated, and the significant differences were then tested with BH-FDR correction. The directed connectivity between different cerebral regions of DP and HC is shown in Fig. 6.

Fig. 2 Mean weighted directed brain network graph of **a** healthy controls and **b** depressive patients. In order to facilitate observation, the connection weights between channels greater than 0.172 are retained

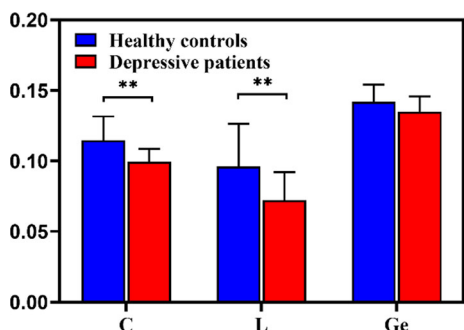
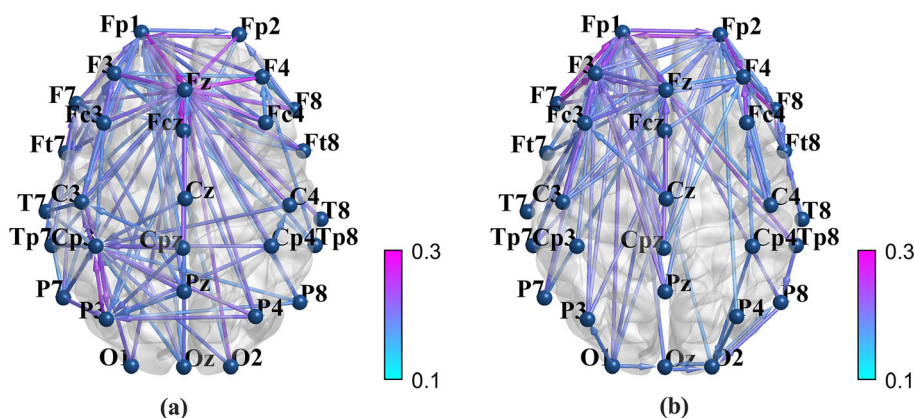


Fig. 3 Topological parameters of directed functional networks in healthy controls (blue) and depressive patients (red). The mean and standard deviation are represented by bars and lines, respectively. The significant differences in the network properties between the two groups are denoted by double asterisks (corrected $p < .01$)

We found significant decreased connectivity in the frontal-to-central (FC, 6.6274 ± 1.7606 versus 8.5031 ± 1.8066 , $t = 3.2836$, corrected $p = .0056$), parietal-to-central (PC, 5.3759 ± 1.6513 versus 6.3801 ± 0.8354 , $t =$

2.3776 , corrected $p = .0312$), and occipital-to-central (OC, 2.9986 ± 1.1553 versus 3.7121 ± 0.5514 , $t = 2.4406$, corrected $p = .0312$) regions existed in DP. Besides, the connectivity strength in the temporal-to-central (TC, 6.3751 ± 1.8356 versus 1.8356 ± 1.4711 , $t = 2.3739$, corrected $p = .0583$) regions also tended to show a lower value in DP. In general, the disrupted connectivity was mainly presented in the information flowing into the central parts, which may indicate that the central parts in depressive groups served as the local hubs appear to lose the function of integrating various types of sensory, cognitive and emotional information from other parts.

Local topological parameters

To investigate the dysfunction of DP in local brain regions, the strength, out-strength, in-strength, and local efficiency of each subject were computed and compared between two

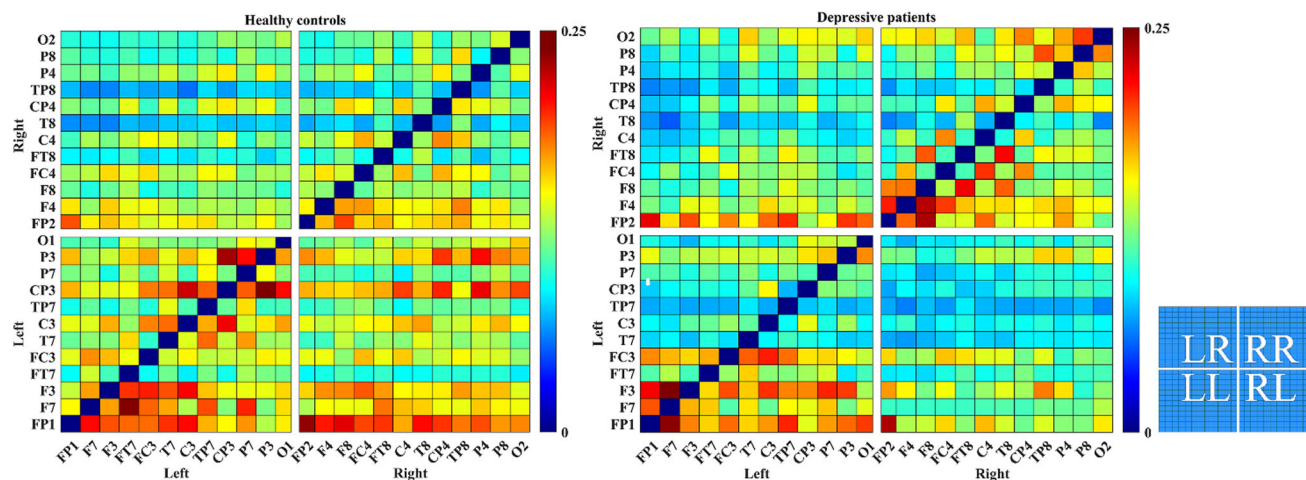


Fig. 4 The mean weighted PDC matrices of different groups. Each matrix consists of four parts, representing the inter-hemispheric and the intra-hemispheric connectivity. The color bar is shown at the right of each matrix. The capital letters in the four quadrants of the small

matrix mean left-to-left hemisphere (LL), left-to-right hemisphere (LR), right-to-right hemisphere (RR), and right-to-left hemisphere (RL), respectively

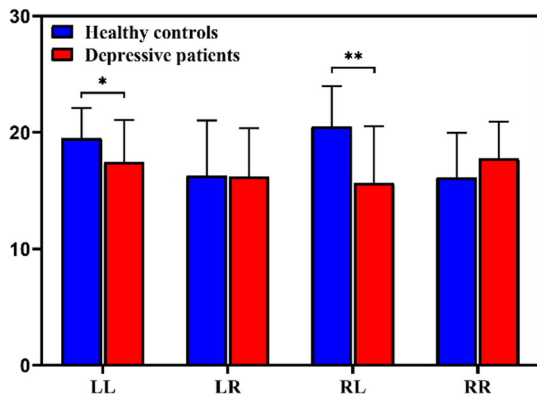
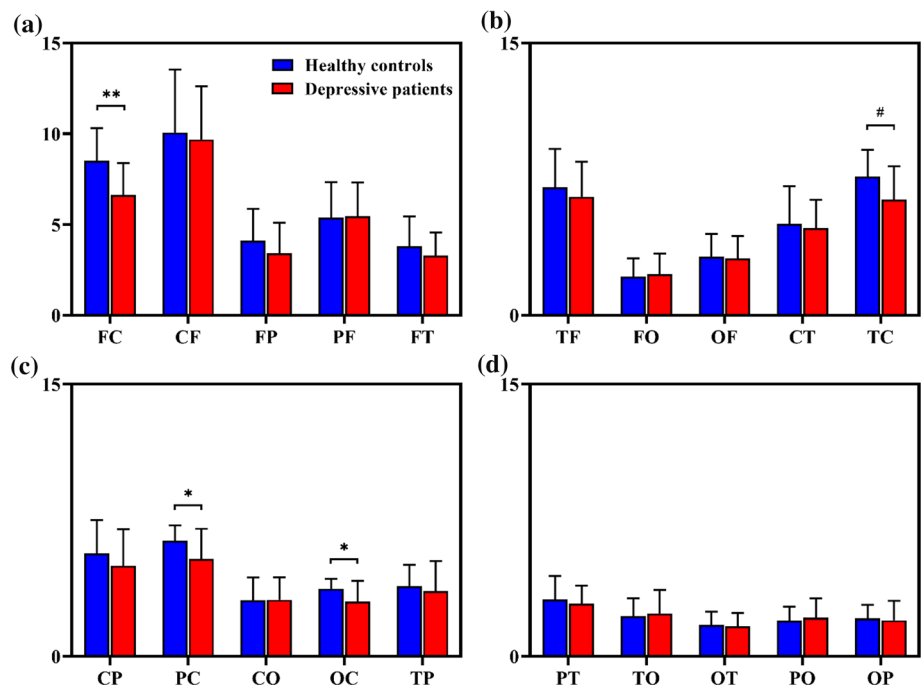


Fig. 5 The inter-hemispheric (LR, RL) and intra-hemispheric (LL, RR) connectivity of healthy controls and depressive patients. The mean and standard deviation are represented by bars and lines, respectively, with blue for healthy controls and red for depressive patients. The asterisks denote corrected $p < .05$ (t-test) and double asterisks denote corrected $p < .01$ (t-test) after correction

groups. The significant differences after correction were highlighted by the bold words.

As presented in Table 1, both the strength and local efficiency of nodes located in central regions were lower in DP than HC. Furthermore, we found that the out-strength and local efficiency of frontal, occipital and parietal nodes were lower in DP. However, the significant difference of in-strength was only shown in C3 node. All these local findings indicate the abnormalities of functional segregation in DP, while functional segregation is important to specialized processing in brain (Mikail Rubinov and Sporns 2010).

Fig. 6 The directed connectivity of healthy controls and depressive patients between different regions. F, T, C, P, and O indicate frontal, temporal, central, parietal, and occipital, respectively. Combinations of different letters indicate directed connectivity between different regions (e.g. FC means frontal to central regions). The mean and standard deviation are represented by bars and lines, respectively, with blue for healthy controls and red for depressive patients. The asterisks denote corrected $p < .05$ (t-test) and double asterisks denote corrected $p < .01$ (t-test) and octothorpes denote corrected $p < .06$ (t-test)



Correlation with HDRS scores

To explore the correlations between the network metrics and clinical symptoms of depressive patients, Pearson correlation analysis and linear regression were performed between the network metrics (C , L) and HDRS scores as well as the directed connectivity (LL, RL) and HDRS scores at alpha frequency band in the EC state. All of these metrics in depressive patients were significantly different from that in healthy controls. Correlation coefficients between HDRS scores and LL and RL were significant after correction ($LL : r = -0.5142, \text{corrected } p = 0.0381, RL : r = -0.4787, \text{corrected } p = 0.0381$). This finding indicate that the severity of depressive symptoms was negatively correlated with the intra- and inter-hemispheric connectivity.

Discussion

In this study, we used partial directed coherence and graph theoretic analysis to investigate the differences of weighted directed brain network between DP and HC. We constructed the weighted directed brain network at alpha, beta, and gamma frequency bands in eyes-closed and eyes-open states. Topological characteristics and weighted directed functional connectivity were compared to find the hypo-function of brain network in DP. Our results indicated obvious alteration at the alpha band in the eyes-closed state.

Table 1 Local topological parameters including strength, out-strength, in-strength, and local efficiency of different groups

	Healthy controls (n = 20)	Depressive patients (n = 19)	Corrected p value		Healthy controls (n = 20)	Depressive patients (n = 19)	Corrected p value
<i>The strength of different groups</i>							
FP1	9.08	8.38	0.4539	C4	7.53	6.67	0.1652
FP2	8.16	8.15	0.6051	T8	6.24	5.89	0.2664
F7	8.28	6.83	0.0944	TP7	7.23	6.06	0.1238
F3	8.36	8.23	0.5562	CP3	9.04	6.79	0.0944
FZ	9.68	8.31	0.1652	CPZ	7.89	7.01	0.1652
F4	7.88	8.01	0.6277	CP4	7.68	6.92	0.1761
F8	7.30	7.09	0.5146	TP8	6.26	6.16	0.5287
FT7	6.98	6.68	0.4611	P7	7.39	6.53	0.1761
FC3	7.82	7.88	0.6051	P3	8.59	7.56	0.2417
FCZ	7.57	7.07	0.2318	PZ	7.53	6.74	0.1652
FC4	7.76	7.06	0.1652	P4	7.57	6.73	0.1652
FT8	6.72	6.94	0.6818	P8	7.09	7.19	0.6277
T7	7.64	6.36	0.1238	O1	7.63	6.70	0.1238
C3**	8.17	6.41	0.0022	OZ	7.17	7.19	0.6051
CZ	7.52	6.51	0.1238	O2	7.16	7.67	0.7580
<i>The out-strength of different groups</i>							
FP1	3.64	3.27	0.0539	C4	3.82	3.51	0.0811
FP2*	3.68	3.26	0.0314	T8*	4.03	3.68	0.0349
F7	3.65	3.34	0.0811	TP7*	4.00	3.72	0.0459
F3	3.60	3.18	0.0557	CP3	3.83	3.84	0.5270
FZ	3.48	3.19	0.0869	CPZ*	3.89	3.61	0.0459
F4*	3.75	3.29	0.0459	CP4*	3.90	3.52	0.0459
F8**	3.99	3.38	0.0051	TP8*	4.07	3.75	0.0314
FT7*	4.03	3.63	0.0314	P7	3.99	3.70	0.0557
FC3	3.72	3.37	0.0516	P3	3.79	3.58	0.1881
FCZ	3.78	3.42	0.0811	PZ	3.99	3.72	0.0811
FC4*	3.86	3.44	0.0459	P4	3.91	3.60	0.0563
FT8*	3.99	3.53	0.0280	P8	3.97	3.70	0.0654
T7	3.92	3.81	0.2341	O1	3.88	3.71	0.1482
C3	3.71	3.62	0.3103	OZ*	3.91	3.51	0.0314
CZ*	3.80	3.42	0.0459	O2*	3.89	3.55	0.0459
<i>The in-strength of different groups</i>							
FP1	5.44	5.12	0.6735	C4	3.72	3.16	0.4675
FP2	4.48	4.88	0.8489	T8	2.21	2.21	0.7993
F7	4.63	3.49	0.3143	TP7	3.22	2.33	0.3605
F3	4.76	5.05	0.8489	CP3	5.21	2.94	0.2235
FZ	6.2	5.12	0.4675	CPZ	4.00	3.40	0.4675
F4	4.13	4.73	0.8598	CP4	3.78	3.40	0.5274
F8	3.30	3.72	0.8489	TP8	2.19	2.40	0.8489
FT7	2.95	3.05	0.8411	P7	3.40	2.83	0.4675
FC3	4.11	4.50	0.8489	P3	4.80	3.98	0.4800
FCZ	3.79	3.65	0.6735	PZ	3.54	3.01	0.4675
FC4	3.90	3.61	0.5679	P4	3.67	3.13	0.4675
FT8	2.73	3.41	0.8927	P8	3.12	3.49	0.8489
T7	3.72	2.55	0.3030	O1	3.75	2.99	0.3605
C3*	4.46	2.79	0.0210	OZ	3.26	3.69	0.8489
CZ	3.72	3.08	0.4675	O2	3.27	4.13	0.8780

Table 1 (continued)

	Healthy controls (n = 20)	Depressive patients (n = 19)	Corrected <i>p</i> value		Healthy controls (n = 20)	Depressive patients (n = 19)	Corrected <i>p</i> value
<i>The local efficiency of different groups</i>							
FP1	0.1275	0.1129	0.0837	C4*	0.1171	0.1013	0.0167
FP2	0.1219	0.1128	0.1645	T8	0.1033	0.0948	0.1021
F7*	0.1228	0.1033	0.0167	TP7*	0.1149	0.0958	0.0167
F3	0.1248	0.1123	0.0587	CP3**	0.1283	0.1044	0.0046
FZ**	0.1345	0.1136	0.0081	CPZ*	0.1229	0.1070	0.0239
F4	0.1203	0.1137	0.1645	CP4*	0.1203	0.1037	0.0167
F8	0.1157	0.1056	0.1011	TP8	0.1040	0.0980	0.1645
FT7	0.1127	0.1011	0.0837	P7*	0.1174	0.1003	0.0167
FC3	0.1211	0.1114	0.1317	P3*	0.1245	0.1102	0.0416
FCZ*	0.1168	0.1055	0.0254	PZ*	0.1182	0.1042	0.0254
FC4*	0.1199	0.1066	0.0278	P4*	0.1199	0.1033	0.0167
FT8	0.1096	0.1041	0.2275	P8	0.1143	0.1072	0.1645
T7*	0.1193	0.0997	0.0167	O1*	0.1194	0.1046	0.0199
C3***	0.1239	0.1011	0.0007	OZ	0.1148	0.1070	0.1314
CZ*	0.1172	0.1013	0.0167	O2	0.1157	0.1093	0.1645

*Corrected $p < 0.05$ **Corrected $p < 0.01$ ***Corrected $p < 0.001$

The significant differences after correction were highlighted by the bold words

Actually, abnormal alpha oscillations in depression have been repeatedly reported in many earlier studies (Fingelkurts et al. 2007; Gotlib et al. 1998; Zhang et al. 2018), but they have not yielded unified conclusions. We speculated that the inconsistent results may be caused by different brain patterns in different resting states including eyes-open and eyes-closed. Studies have also reported that brain in resting state maintains different patterns in eyes-open and eyes-closed condition, especially for alpha oscillations (Robert et al. 2007). Consequently, we designed the 8 min resting state experiment with eyes open and eyes closed in two alternating orders by voice playback, and analyzed eyes-open and eyes-closed states under different frequency bands. It was at the alpha frequency band in eyes-closed state that we found the most obvious alteration between DP and HC, thus we present our further results at alpha band in EC state only.

The results of topological characteristics showed decreased C and L in DP. Previous studies that used unweighted and undirected networks have reported lower C (Li et al. 2015; Sun et al. 2019; Zhang et al. 2018) and L (Hasanzadeh et al. 2020; Leistedt et al. 2009; Sun et al. 2019; Zhang et al. 2018) in patients with depression compared with healthy controls. It is stated that these alterations indicate a more random structure of depressive

patients (Latora and Marchiori 2001), namely random network. Our observed more random network in depressive patients was consistent with these studies. This random structure in depressive patients is assumed to affect the cognitive capability of brain (Leistedt et al. 2009) and related to the abnormal changes of network hubs (Zhang et al. 2018). Random networks also show less modularized information processing capability or fault tolerance (Latora and Marchiori 2001; Zhang et al. 2011).

As mentioned above, to our knowledge, the weighted directed brain network has not been systematically tested in depression. The current study based on PDC is an attempt to expand the research on the weighted directed brain network in patients with depression. PDC is a promising tool that is better able to deal with multichannel data and identify the causality of interdependence between electrodes compared with conventional spectrum-based EEG analysis, thus providing more details of cortical functional interactions (Sun et al. 2008). Because the value of PDC can represent the direction between electrodes, we constructed the directed brain network, which was able to indicate the causality between brain regions. As the results showed in Fig. 5, the inter-hemispheric interactions (right-to-left) and the intra-hemispheric interactions (left-to-left) in depressed patients decreased significantly. Many earlier

studies suggested that communication between the left and right cerebral hemispheres is a crucial component of cognitive and emotional processing (Banich et al. 1992; Compton et al. 2005; Toro et al. 2008). Inter-hemispheric communication of information is important for several reasons: to ensure that each hemisphere has access to crucial perceptual information about the world; and to allow for complex cognitive tasks to be allocated between the hemispheres in a manner that takes advantage of the cognitive specializations of each hemisphere (Banich et al. 1992). Thus, the result of decreased connectivity of the right-to-left hemisphere may cause an imbalance of information transmission between hemispheres, especially for right-to-left hemispheres. This abnormality in information processing of DP is consistent with a previous study that reported asymmetry to the left hemisphere, which interpreted as a cortical deactivation of the right cerebral hemisphere and seems to be a state marker of depression (Haag et al. 1994; Henriques et al. 1991). A study based on fMRI of depressed patients also found deficits in the interhemispheric connectivity in depressed patients (Wang et al. 2013).

The electrode activities of the midline were also considered. The connectivity strengths of the inner midline (MM), left hemisphere to midline (LM), midline to left hemisphere (ML), right hemisphere to midline (RM), and midline to right hemisphere (MR) were calculated. Only connectivity strength of ML was significantly (corrected, $p = 0.02$) decreased in DP, which indicate the dysfunction of the left hemisphere in DP served as the information recipient.

As we can see in Fig. 6, weighted directed decreased connectivity of several specialized regions was presented. FC, PC, OC and TC connectivity was significantly lower in DP compared with HC. Our results also revealed that the outgoing information of the frontal, temporal, occipital and central parts in depressed patients were both decreased, but there was only decreased ingoing information in the left central parts (Table 1). These findings can be considered as a sign of lower information flow from frontal, temporal, occipital and parietal to left central regions in DP. The similar decreased results were also observed in local efficiency in DP, which means abnormality of functional segregation. We speculated that the central parts in depressive groups served as the local hubs appear to lose the function of integrating various types of sensory, cognitive and emotional information from other parts. In fact, cerebral activities have been investigated in the fronto-central and centro-parietal regions in patients with bipolar disorders (BD). A research about EEG alpha band suggest BD patients showed a decrease of mean synchronization in the alpha band, and the decreases were greatest in fronto-central and centro-parietal connections (Kim et al. 2013).

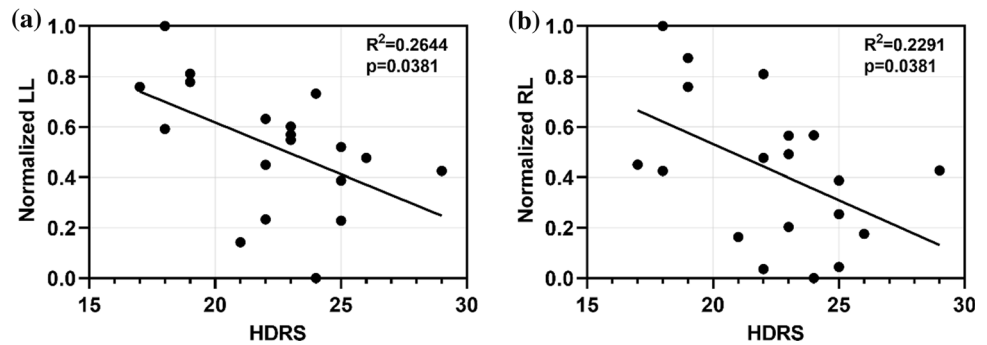
Our findings support the reports about the cognitive decline and emotional disorders of depressed patients, which may provide new evidence about the disruptions of the interactions from frontal, temporal, occipital and parietal to central regions.

What's more, to further highlight the advantages of the directed weighted brain network, we have constructed undirected brain networks using magnitude squared coherence (MSC) as a reference calculated by using HERMES, a toolbox on MATLAB (Niso et al. 2013). MSC measures the linear correlation between two variables $x(t)$ and $y(t)$ as a function of the frequency, f . We computed the same network metrics as we did earlier, and no significant results after correction were found. We found no statistical differences at any frequency band in EC or EO state ($p = 0.74, 0.23, 0.09, 0.46, 0.46$ and 0.24 corresponding to alpha.EC, beta.EC, gamma.EC, alpha.EO, beta.EO and gamma.EO, respectively). Specifically, at alpha band in EC state, differences of the connectivity between the two hemispheres ($p = 0.64$) and within the left hemisphere ($p = 0.66$), as well as differences of the connectivity between different cerebral (frontal, temporal, occipital, parietal) regions and the central regions ($p > 0.05$) and differences in topological characteristics ($p = 0.74, 0.70$ and 0.74 corresponding to C , L and G_e , respectively), found in the directed network, did not appear in the undirected network. We speculated that undirected networks may confuse the direction of information flow in brain and lose the essential information in DP. Providing more useful information, directed brain networks can be considered as more effective tools for exploring the neurophysiological mechanisms of psychiatric disorders such as depression.

Figure 7 shows that the severity of DP is negatively correlated with two measured network metrics (LL and RL). DP with attenuated left to left and right to left hemispheric connectivity may have higher HDRS scores, indicating that the lower the LL and RL , the more severe the depression.

There are some limitations in our study. It must be acknowledged that the gamma rhythm is one of the popular approaches in studying neuromarkers of depression. Gamma rhythms are correlated with increased neuronal action potential generation (Nir et al. 2007; Watson et al. 2018). Many studies have indicated that gamma rhythms of HC are different from that of depressive patients (Akar et al. 2015; Lee et al. 2010; Liao et al. 2017; Liu et al. 2014; Pizzagalli et al. 2006; Siegle et al. 2010; Strelets et al. 2007). For example, an EEG study found that subjects with high depression scores (including Beck Depression Inventory (BDI) and Mood and Anxiety Symptom Questionnaire (MASQ) scores) had reduced resting gamma in the anterior cingulate cortex, whereas gamma increased in

Fig. 7 Correlation between HDRS scores and **a** normalized left to left hemispheric connectivity (*LL*), and **b** normalized right to left hemispheric connectivity (*RL*)



frontal and temporal regions in a study in which subjects with depression performed spatial and arithmetic tasks (Pizzagalli et al. 2006). In addition, subjects performing emotion-related tasks in major depression can show decreased frontal cortex gamma (Lee et al. 2010; Liu et al. 2014). Akar et al. found increased resting complexity of gamma signaling in the frontal and parietal cortex in subjects with major depression. All these studies prove that gamma rhythms are an important direction to explore the alterations of the brain in DP compared with healthy controls (Akar et al. 2015). However, we did not find significant differences at the gamma band. A possible reason is that we didn't include cognitive tasks for DP. Our future study will further address the task-specific and sensory-based approaches for gamma rhythms. Besides, the number of subjects needed to be increased to make our results more convincing and we are working to recruit more subjects for further research.

In summary, we found decreased connectivity in DP at the alpha band during resting state with eyes closed. In addition, lower clustering coefficients and characteristic path lengths in DP indicate a more randomized network structure. Furthermore, the reduced inter-hemispheric (right-to-left) and intra-hemispheric (left-to-left) functional connectivity of DP suggest that DP have imbalance of information transmission coordination from right-to-left hemisphere, which may inhibit the expression of cognitive function. The decreased interaction from frontal to central, temporal to central, parietal to central and occipital to central in depressed patients suggest that the central parts in DP served as the local hubs appear to lose the function of integrating various types of sensory, cognitive and emotional information from other parts. Local findings including local efficiency and out-strength indicate the abnormalities of functional segregation in DP, while functional segregation is important to specialized processing in brain. What's more, the directed network metrics may reflect an effective measure of the severity of depression. Based on our findings, we speculate that our research may serve as a potential neuromarker of the severity of depression.

Acknowledgements The authors thanked all the participants in this study. This work was supported by the National Key Research and Development Program of China under Grant 2017YFB1002504, National Natural Science Foundation of China (No. 81925020, 81630051, 81801786).

Data availability Data are available on request to the authors.

Declarations

Conflict of interest The authors declare that they have no known competing financial interests or personal relationships that could have appeared to influence the work reported in this paper.

Open Access This article is licensed under a Creative Commons Attribution 4.0 International License, which permits use, sharing, adaptation, distribution and reproduction in any medium or format, as long as you give appropriate credit to the original author(s) and the source, provide a link to the Creative Commons licence, and indicate if changes were made. The images or other third party material in this article are included in the article's Creative Commons licence, unless indicated otherwise in a credit line to the material. If material is not included in the article's Creative Commons licence and your intended use is not permitted by statutory regulation or exceeds the permitted use, you will need to obtain permission directly from the copyright holder. To view a copy of this licence, visit <http://creativecommons.org/licenses/by/4.0/>.

References

- Achard S, Bullmore E (2007) Efficiency and cost of economical brain functional networks. *PLoS Comput Biol* 3(2):e17. <https://doi.org/10.1371/journal.pcbi.0030017>
- Akar SA, Kara S, Agambayev S, Bilgic V (2015) Nonlinear analysis of EEG in major depression with fractal dimensions. *Conf Proc IEEE Eng Med Biol Soc 2015:7410–7413*. <https://doi.org/10.1109/embc.2015.7320104>
- Baccalá L, Sameshima KJBC (2001) Partial directed coherence: a new concept in neural structure determination. *Biol Cybern* 84(6):463–474
- Banich MT, Karol DLJJOEPHP (1992) The sum of the parts does not equal the whole: evidence from bihemispheric processing. *J Exp Psychol Hum Percept Perform* 18(3):763. <https://doi.org/10.1037//0096-1523.18.3.763>
- Barry RJ, Clarke AR, Johnstone SJ, Magee CA, Rushby JA (2007) EEG differences between eyes-closed and eyes-open resting conditions. *Clin Neurophysiol*. <https://doi.org/10.1016/j.clinph.2007.07.028>

- Bassett DS, Bullmore E (2006) Small-world brain networks. *Neuroscientist* 12(6):512–523. <https://doi.org/10.1177/1073858406293182>
- Benjamini Y, Hochberg YJOTRSSSBM (1995) Controlling the false discovery rate: a practical and powerful approach to multiple testing. *J R Stat Soc Ser B (methodological)* 57(1):289–300. <https://doi.org/10.1111/j.2517-6161.1995.tb02031.x>
- Bertini M, Ferrara M, De Gennaro L, Curcio G, Moroni F, Vecchio F, De Gasperis M, Rossini PM, Babiloni C (2007) Directional information flows between brain hemispheres during presleep wake and early sleep stages. *Cereb Cortex* 17(8):1970–1978. <https://doi.org/10.1093/cercor/bhl106>
- Bullmore E, Sporns O (2009) Complex brain networks: graph theoretical analysis of structural and functional systems. *Nat Rev Neurosci* 10(3):186–198. <https://doi.org/10.1038/nrn2575>
- Coito A, Michel CM, Mierlo PV, Vulliemoz S, Plomp G (2016) Directed functional brain connectivity based on EEG source imaging: methodology and application to temporal lobe epilepsy. *IEEE Trans Biomed Eng* 63(12):2619–2628. <https://doi.org/10.1109/TBME.2016.2619665>
- Coito A, Michel CM, Vulliemoz S, Plomp G (2019) Directed functional connections underlying spontaneous brain activity. *Hum Brain Mapp* 40(3):879–888. <https://doi.org/10.1002/hbm.24418>
- Cole MW, Repovš G, Anticevic A (2014) The frontoparietal control system: a central role in mental health. *Neuroscientist* 20(6):652–664. <https://doi.org/10.1177/1073858414525995>
- Compton RJ, Feigenson K, Widick PJCBR (2005) Take It to the bridge: an interhemispheric processing advantage for emotional faces. *Cogn Brain Res* 24(1):66–72. <https://doi.org/10.1016/j.cogbrainres.2004.12.002>
- DeRubeis RJ, Siegle GJ, Hollon SD (2008) Cognitive therapy versus medication for depression: treatment outcomes and neural mechanisms. *Nat Rev Neurosci* 9(10):788–796. <https://doi.org/10.1038/nrn2345>
- Fagiolo G (2007) Clustering in complex directed networks. *Phys Rev E* 76(2):026107. <https://doi.org/10.1103/PhysRevE.76.026107>
- Fingelkurts AA, Fingelkurts AA, Rytysälä H, Suominen K, Isometsä E, Kähkönen S (2007) Impaired functional connectivity at EEG alpha and theta frequency bands in major depression. *Hum Brain Mapp* 28(3):247–261. <https://doi.org/10.1002/hbm.20275>
- Gotlib I (1998) EEG alpha asymmetry, depression, and cognitive functioning. *Cogn Emot* 12(3):449–478
- Haag C, Kathmann N, Hock C, Günther W, Voderholzer U, Laakmann GJBP (1994) Lateralization of the Bereitschaftspotential to the left hemisphere in patients with major depression. *Biol Psychiatry* 36(7):453. [https://doi.org/10.1016/0006-3223\(94\)90640-8](https://doi.org/10.1016/0006-3223(94)90640-8)
- Hasanzadeh F, Mohebbi M, Rostami R (2020) Graph theory analysis of directed functional brain networks in major depressive disorder based on EEG signal. *J Neural Eng* 17(2):026010. <https://doi.org/10.1088/1741-2552/ab7613>
- Henriques JB, Davidson RJ (1991) Left frontal hypoactivation in depression. *J Abnorm Psychol*. <https://doi.org/10.1037/0021-843X.100.4.535>
- Hulshoff Pol H, Bullmore E (2013) Neural networks in psychiatry. *Eur Neuropsychopharmacol* 23(1):1–6. <https://doi.org/10.1016/j.euroneuro.2012.12.004>
- Kaiser M (2011) A tutorial in connectome analysis: topological and spatial features of brain networks. *Neuroimage* 57(3):892–907. <https://doi.org/10.1016/j.neuroimage.2011.05.025>
- Kessler RC, Berglund P, Demler O, Jin R, Koretz D, Merikangas KR, Rush AJ, Walters EE, Wang PS (2003) The epidemiology of major depressive disorder results from the national comorbidity survey replication (NCS-R). *JAMA* 289(23):3095–3105. <https://doi.org/10.1001/jama.289.23.3095>
- Kim DJ, Bolbecker AR, Howell J, Rass O, Sporns O, Hetrick WP, Breier A, O'Donnell BF (2013) Disturbed resting state EEG synchronization in bipolar disorder: a graph-theoretic analysis. *NeuroImage Clin* 2:414–423. <https://doi.org/10.1016/j.nicl.2013.03.007>
- Klimesch W (1999) EEG alpha and theta oscillations reflect cognitive and memory performance: a review and analysis. *Brain Res Rev* 29(2):169–195. [https://doi.org/10.1016/S0165-0173\(98\)00056-3](https://doi.org/10.1016/S0165-0173(98)00056-3)
- Latora V, Marchiori MJPRL (2001) Efficient behavior of small-world. *Networks* 87(19):198701. <https://doi.org/10.1103/PhysRevLett.87.198701>
- Lee PS, Chen YS, Hsieh JC, Su TP, Chen LF (2010) Distinct neuronal oscillatory responses between patients with bipolar and unipolar disorders: a magnetoencephalographic study. *J Affect Disord* 123(1–3):270–275. <https://doi.org/10.1016/j.jad.2009.08.020>
- Leistedt SJ, Coumans N, Dumont M, Lanquart JP, Stam CJ, Linkowski P (2009) Altered sleep brain functional connectivity in acutely depressed patients. *Hum Brain Mapp* 30(7):2207–2219. <https://doi.org/10.1002/hbm.20662>
- Li Y, Cao D, Wei L, Tang Y, Wang J (2015) Abnormal functional connectivity of EEG gamma band in patients with depression during emotional face processing. *Clin Neurophysiol* 126(11):2078–2089. <https://doi.org/10.1016/j.clinph.2014.12.026>
- Li H, Zhou H, Yang Y, Wang H, Zhong N (2017) More randomized and resilient in the topological properties of functional brain networks in patients with major depressive disorder. *J Clin Neurosci* 44:274–278. <https://doi.org/10.1016/j.jocn.2017.06.037>
- Liao SC, Wu CT, Huang HC, Cheng WT, Liu YH (2017) Major depression detection from EEG signals using kernel eigen-filter-bank common spatial patterns. *Sensors (basel)*. <https://doi.org/10.3390/s17061385>
- Liu TY, Chen YS, Su TP, Hsieh JC, Chen LF (2014) Abnormal early gamma responses to emotional faces differentiate unipolar from bipolar disorder patients. *Biomed Res Int* 2014:906104. <https://doi.org/10.1155/2014/906104>
- Meng C, Brandl F, Tahmasian M, Shao J, Manoliu A, Scherr M, Schwerthöffer D, Bäuml J, Förstl H, Zimmer C, Wohlschläger AM (2014) Aberrant topology of striatum's connectivity is associated with the number of episodes in depression. *Brain* 137(Pt 2):598–609. <https://doi.org/10.1093/brain/awt290>
- Micheloyannis S, Pachou E, Stam CJ, Breakspear M, Bitsios P, Vourkas M, Erimaki S, Zervakis M (2006) Small-world networks and disturbed functional connectivity in schizophrenia. *Schizophr Res* 87(1):60–66. <https://doi.org/10.1016/j.schres.2006.06.028>
- Mognon A, Jovicich J, Bruzzone L, Buiatti M (2011) ADJUST: an automatic EEG artifact detector based on the joint use of spatial and temporal features. *Psychophysiology* 48(2):229–240. <https://doi.org/10.1111/j.1469-8986.2010.01061.x>
- Nir Y, Fisch L, Mukamel R, Gelbard-Sagiv H, Arieli A, Fried I, Malach R (2007) Coupling between neuronal firing rate, gamma LFP, and BOLD fMRI is related to interneuronal correlations. *Curr Biol* 17(15):1275–1285. <https://doi.org/10.1016/j.cub.2007.06.066>
- Niso G, Bruña R, Pereda E, Gutiérrez R, Bajo R, Maestú F, del Pozo F (2013) HERMES: towards an integrated toolbox to characterize functional and effective brain connectivity. *Neuroinformatics* 11(4):405–434. <https://doi.org/10.1007/s12021-013-9186-1>
- Park CH, Wang SM, Lee HK, Kweon YS, Lee CT, Kim KT, Kim YJ, Lee KU (2014) Affective state-dependent changes in the brain functional network in major depressive disorder. *Soc Cogn Affect Neurosci* 9(9):1404–1412. <https://doi.org/10.1093/scan/nst126>
- Pizzagalli DA, Peccoralo LA, Davidson RJ, Cohen JD (2006) Resting anterior cingulate activity and abnormal responses to errors in

- subjects with elevated depressive symptoms: a 128-channel EEG study. *Hum Brain Mapp* 27(3):185–201. <https://doi.org/10.1002/hbm.20172>
- Rubinov M, Sporns O (2010) Complex network measures of brain connectivity: uses and interpretations. *Neuroimage* 52(3):1059–1069. <https://doi.org/10.1016/j.neuroimage.2009.10.003>
- Rubinov M, Knock SA, Stam CJ, Micheloyannis S, Harris AW, Williams LM, Breakspear M (2009) Small-world properties of nonlinear brain activity in schizophrenia. *Hum Brain Mapp* 30(2):403–416. <https://doi.org/10.1002/hbm.20517>
- Sameshima K, Baccalá LA (1999) Using partial directed coherence to describe neuronal ensemble interactions. *J Neurosci Methods* 94(1):93–103. [https://doi.org/10.1016/S0165-0270\(99\)00128-4](https://doi.org/10.1016/S0165-0270(99)00128-4)
- Schnieder T, Neumaier AJATOMS (2001) Algorithm 808: Arfit - a Matlab package for the estimation of parameters and eigenmodes of multivariate autoregressive models. *ACM Trans Math Softw* 27:58–65
- Siegle GJ, Condray R, Thase ME, Keshavan M, Steinhauer SR (2010) Sustained gamma-band EEG following negative words in depression and schizophrenia. *Int J Psychophysiol* 75(2):107–118. <https://doi.org/10.1016/j.ijpsycho.2008.04.008>
- Sperdin HF, Coito A, Kojovic N, Rihs TA, Jan RK, Franchini M, Plomp G, Vulliamoz S, Eliez S, Michel CM, Schaer M (2018) Early alterations of social brain networks in young children with autism. *Elife* 7:e31670. <https://doi.org/10.7554/eLife.31670>
- Stam CJ, Reijneveld JC (2007) Graph theoretical analysis of complex networks in the brain. *Nonlinear Biomed Phys* 1(1):3. <https://doi.org/10.1186/1753-4631-1-3>
- Stam C, Jones B, Nolte G, Breakspear M, Scheltens PJCC (2006) Small-world networks and functional connectivity in Alzheimer's disease. *Cereb Cortex*. <https://doi.org/10.1093/cercor/bhj127>
- Stam CJ, De Haan W, Daffertshofer AB, Jones BF, Manshanden I, van Cappellen van Walsum AM, Montez T, Verbunt JP, De Munck JC, Van Dijk BW, Berendse HW (2008) Graph theoretical analysis of magnetoencephalographic functional connectivity in Alzheimer's disease. *Brain* 132(1):213–224. <https://doi.org/10.1093/brain/awn262>
- Strakowski SM, Adler CM, Almeida J, Altshuler LL, Blumberg HP, Chang KD, DelBello MP, Frangou S, McIntosh A, Phillips ML, Sussman JE (2012) The functional neuroanatomy of bipolar disorder: a consensus model. *Bipolar Disord* 14(4):313–325. <https://doi.org/10.1111/j.1399-5618.2012.01022.x>
- Strelets VB, Garakh Zh V, Novototskii-Vlasov VY (2007) Comparative study of the gamma rhythm in normal conditions, during examination stress, and in patients with first depressive episode. *Neurosci Behav Physiol* 37(4):387–394. <https://doi.org/10.1007/s11055-007-0025-4>
- Sun Y, Li Y, Zhu Y, Chen X, Tong S (2008) Electroencephalographic differences between depressed and control subjects: an aspect of interdependence analysis. *Brain Res Bull* 76(6):559–564. <https://doi.org/10.1016/j.brainresbull.2008.05.001>
- Sun S, Li X, Zhu J, Wang Y, La R, Zhang X, Hu B (2019) Graph theory analysis of functional connectivity in major depression disorder with high-density resting state EEG data. *IEEE Trans Neural Syst Rehabil Eng* 27(3):429–439. <https://doi.org/10.1109/TNSRE.2019.2894423>
- Toro R, Fox PT, Paus T (2008) Functional coactivation map of the human brain. *Cereb Cortex* 18(11):2553–2559. <https://doi.org/10.1093/cercor/bhn014>
- van den Heuvel MP, Hulshoff Pol HE (2010) Exploring the brain network: a review on resting-state fMRI functional connectivity. *Eur Neuropsychopharmacol* 20(8):519–534. <https://doi.org/10.1016/j.euroneuro.2010.03.008>
- Wang L, Li K, Zhang QE, Zeng YW, Jin Z, Dai WJ, Su YA, Wang G, Tan YL, Yu X, Si TM (2013) Interhemispheric functional connectivity and its relationships with clinical characteristics in major depressive disorder: a resting state fMRI study. *PLoS ONE* 8(3):e60191. <https://doi.org/10.1371/journal.pone.0060191>
- Watson BO, Ding M, Buzsáki G (2018) Temporal coupling of field potentials and action potentials in the neocortex. *Eur J Neurosci* 48(7):2482–2497. <https://doi.org/10.1111/ejn.13807>
- Zhang J, Wang J, Wu Q, Kuang W, Huang X, He Y, Gong Q (2011) Disrupted brain connectivity networks in drug-naive, first-episode major depressive disorder. *Biol Psychiat* 70(4):334–342. <https://doi.org/10.1016/j.biopsych.2011.05.018>
- Zhang M, Zhou H, Liu L, Feng L, Yang J, Wang G, Zhong N (2018) Randomized EEG functional brain networks in major depressive disorders with greater resilience and lower rich-club coefficient. *Clin Neurophysiol* 129(4):743–758. <https://doi.org/10.1016/j.clinph.2018.01.017>

Publisher's Note Springer Nature remains neutral with regard to jurisdictional claims in published maps and institutional affiliations.